平成 24 年度

三重大学大学院　生物資源学研究科

修士論文

Hemispheric hot summer in 2010 and its relation to the Arctic Oscillation and the Atlantic Ocean

北大西洋の海面水温パターンがもたらす北極振動の極性反転と 2010 年猛暑

Climate and Ecosystems Dynamics Division

Graduate school of Bioresources

Mie University

511M222

Yuriko Otomi

Supervisor: Prof. Yoshihiro Tachibana

March 4, 2013

Abstract

In 2010, the Northern Hemisphere, in particular Russia, Europe and Japan, experienced an abnormally hot summer characterized by record-breaking warm temperatures and associated with a strongly positive Arctic Oscillation (AO), that is, low pressure in the Arctic and high pressure in the midlatitudes. In contrast, in winter 2009/2010, just a half-year earlier, Eurasian continent suffered from anomalously cold weather associated with a record-breaking negative AO, indicating that AO index abruptly changed from strong negative to strong positive. The abrupt change of AO index in 2010 corresponded to the change from the abnormally cold winter of 2009/2010 to the abnormally hot summer of 2010. The AO polarity reversal that began in summer 2010 can explain the abnormally hot summer. The winter sea surface temperatures (SST) in the North Atlantic Ocean showed a tripolar anomaly pattern—warm SST anomalies over the tropics and high latitudes and cold SST anomalies over the midlatitudes—under the influence of the negative AO. The warm SST anomalies continued into summer 2010 because of the large oceanic heat capacity. A AGCM (atmospheric general circulation model) simulation strongly suggested that the AO related summertime North Atlantic warm SST anomalies remotely caused the occurrence of the positive summertime AO. Thus, a possible cause of the AO polarity reversal can be the ‘‘memory’’ of the negative winter AO in the North Atlantic Ocean. An interseasonal linkage of the AO probably induces a positive AO in the following summer. Understanding of this interseasonal linkage can aid in the longterm prediction of such abnormal summer events.

Contents

1. Introduction…….4

2. Data and method……..6

3. Result……...9

3.1. The analysis by reanalysis data sets

3.1.1. Strongly positive AO days

3.1.2. Oceanic footprint left by the previous winter's negative AO

3.2. Steady responses to the oceanic forcing in the Atlantic region

3.2.1. AO reproducibility of the AGCM EOF analysis

3.2.2. The response of the atmosphere by North Atlantic SST

4. Discussion……..14

Acknowledgment…….17

References……...18

Figure captions……21

1. Introduction

In Japan, summer 2010 was the warmest in about 100 years of countrywide measurement records. Moreover, summer 2010 was abnormally hot on a planetary scale. For example, Europe, especially Eastern Europe and western Russia, experienced record-breaking hot temperatures, attributed to strong atmospheric blocking over the Euro-Russian region from late June to early August (Matsueda 2011). Additionally, Barriopedro et al. (2011) showed that the spatial extent of the record-breaking temperatures of summer 2010 exceeded the area affected by the previous hottest summer of 2003. Heat anomalies covered almost the entire Eurasian continent in 2010. In contrast, in winter 2009/2010, just a half-year earlier, the continent suffered from anomalously cold weather associated with a record-breaking negative Arctic Oscillation (AO), which is characterized by positive sea level pressure anomalies over the Arctic and negative pressure anomalies over the midlatitudes (Thompson and Wallace 2000). Moreover, in the same winter, a record-breaking negative North Atlantic Oscillation (NAO) caused several severe cold spells over northern and western Europe (Cattiaux et al. 2010). In fact, the strongest negative AO index of the past 30 years was observed in December 2009 (Wang and Chen 2010). This drastic reversal from a record-breaking cold winter to a record-breaking hot summer is preserved in our memory. What if, however, that memory could be preserved not only in our minds but also somewhere on the earth? In particular, might a memory of the strongly negative wintertime 2009/2010 AO have been preserved in the ocean, because of its large thermal heat capacity, which could then be recalled the following summer?

The winter-to-summer evolution of the AO index during 2009/2010 can be summarized as follows: a strongly negative wintertime AO index continued until May, after which it abruptly changed, becoming strongly positive in July and continuing so

until the beginning of August. Details of the AO evolution will be described in the following sections. Ogi et al. (2005) pointed out that a strongly positive summertime AO is associated with occurrences of blocking anticyclones, which contributed to the abnormally hot European summer. Trigo et al. (2005) also reported that a blocking anticyclone caused the anomalous hot summer of 2003. The blocking anticyclone over Europe in summer 2003 was shown to be part of a planetary-scale wave train, extending from Europe to eastern Eurasia (Orsolini and Nikulin 2006). The abrupt change of the AO index from strongly negative to strongly positive in 2010 thus corresponded to the change from the abnormally cold winter of 2009/2010 to the abnormally hot summer of 2010, which shows that the AO index is a good indicator of abnormal weather on a planetary-scale, and that extra-seasonal prediction of the AO is a key to long-term forecasting. In this study, we therefore aimed to examine the cause of the 2010 change in the AO from strongly negative to strongly positive by using reanalysis data set and atmospheric general circulation model (AGCM).

2. Data and method

The AO was first defined by Thompson and Wallace (2000) which is based on an invariant empirical orthogonal function (EOF) spatial pattern throughout the year, and Ogi et al. (2004) identified seasonal variations of the Northern Hemisphere annular mode (SV NAM) from 1958 to 2002 by performing an EOF analysis. EOF was applied to a temporal covariance matrix of geopotential height fields for individual calendar months using a zonally averaged monthly geopotential height field from 1,000 to 200 hPa for the area poleward of 40ºN. The daily time series of the SV NAM index is obtained by projecting daily zonal mean geopotential height anomalies onto the EOF of each month. The time series of the SV NAM index shown in Figure 1 is calculated by this method.

Ogi et al. (2004) and Tachibana et al. (2010) demonstrated that in winter, but not in summer, the SV NAM accords well with the AO defined by Thompson and Wallace (2000) and used by the Climate Prediction Center of the U.S. National Oceanic and Atmospheric Administration (NOAA/CPC). Ogi et al. (2005) and Tachibana et al. (2010) also demonstrated that the SV NAM successfully captures anomalous summertime weather conditions associated with blocking anticyclones, such as the hot summer in Europe in 2003, whereas the original AO of Thompson and Wallace (2000), mainly reflects atmospheric variabilities in winter and cannot capture such a hot summer. Therefore, Ogi et al. (2005) redefined the summertime SV NAM as the summer AO. In this study, therefore, we adopted the SV NAM index defined by Ogi et al. (2004) as the AO index, and all references to the AO index in this study mean the SV NAM index.

We used daily data of large-scale atmospheric fields from the National Centers for Environmental Prediction/National Center for Atmospheric Research (NCEP/NCAR) reanalysis data set (Kalnay et al. 1996) to calculate the climatology and

anomalies of the meteorological field (i.e., temperature, geopotential height, and wind velocity). Monthly means of sea surface temperature (SST) data are from the NOAA_ERSST_V3 data set, provided by NOAA/OAR/ESRL PSD (http://www.esrl.noaa.gov/psd/) (Smith et al. 2008; Xue et al. 2003). We used monthly mean latent and sensible heat flux data of the Japan 25 year Reanalysis (JRA-25) and the JMA Climate Data Assimilation System (JCDAS) to examine the atmosphere–ocean interaction (Onogi et al. 2007). Daily and monthly means of outgoing longwave radiation (OLR) are interpolated OLR data provided by NOAA/OAR/ESRL PSD (Liebmann and Smith 1996). Anomaly fields of individual variables are relative to the multi-year mean climatology from 1979 to 2010 for each month.

We also use AGCM to simulate the hot summer of 2010 by using AGCM for Earth Simulator (AFES). The resolution of the AFES is T119L48. The horizontal grid size of T119 is approximately 1º, and it has 48 vertical layers. The calculation time step is 6 minutes. The outputs are averaged every 6 hours. The experimentation was calculated from July to August. The initial data are each monthly average of July from 1979 to 2010. We calculated 32 members ensemble run. The boundary condition of a control run (CTL) is monthly average SST and ice in July and August for 30 years from 1981 to 2010. As sensitivity experiment, we set the anomalous SST distribution occurred in 2010 over the North Atlantic. This experiment refers to AS run in this study. The SST in other oceans is not changed in the AS run, so the boundary condition of AS differs only in the SST in the North Atlantic Ocean (from 95ºW to 40ºE, from EQ to 90ºN, except Mediterranean Sea) from CTL. The SST of the AS is monthly average SST in July and August 2010. We used JRA-25 and JCDAS as the initial data and the boundary data (Fig. 2). We additionally execute other two sensitivity runs; one is that only the high latitude Atlantic SST is as in AS run (from 95ºW to 40ºE, from 52.5ºN to

90ºN, except Mediterranean Sea), the other is that only the low latitude Atlantic SST is as in AS run (from 95ºW to 40ºE, from EQ to 20ºN, except Mediterranean Sea), and the additional runs refer to HAS run and LAS run respectively in this study.

We calculated EOF analysis of the output of the CTL by the same method as SV NAM is calculated for the reanalysis data set. The daily time series of the SV NAM indexes for each CTL, AS, HAS and LAS are obtained by projecting daily zonal mean geopotential height anomalies onto the leading mode of EOF eigenvector of CTL in August. We respectively calculated the difference of AS, HAS and LAS from CTL by the examining the influence of the anomalous SST in the North Atlantic Ocean.

3. Result

3.1. The analysis by reanalysis data sets

3.1.1. Strongly positive AO days

The winter-to-summer evolution of the AO index (Figure 1) showed a strongly negative AO in winter 2009/2010 that lasted through May, followed by an abrupt change to strongly positive values in July and August 2010. In particular, the AO index was extremely positive from 10 July to 4 August 2010, coinciding with a period of abnormally hot days in eastern Europe and the Russian far east. Moreover, the AO index in winter and summer accords well with changes in the temperature anomaly for the Eurasian continent over the same period (Figure 1, lower panel), although the AO index in spring did not accord well with the temperature. Time-mean atmospheric fields during the strongly positive AO period are shown in Figure 3. The temperature anomaly field at 850 hPa shows two obvious exceptionally hot areas, one centered over eastern Europe and the other over the Russian far east. Between these two hot areas, cold anomaly areas can be seen over central Siberia and the Arctic. At 300 hPa, a negative geopotential height anomaly is seen over the Arctic region that elongates southward toward central Siberia, whereas positive anomalies characterize the midlatitudes of the Northern Hemisphere. Over eastern Europe, Mongolia, the Russian far east, and the eastern North Pacific Ocean the positive anomalies are particularly strong. This pattern is very similar to the positive summer AO pattern observed during the unusually hot summer of 2003 (Ogi et al. 2005). In summer 2010, the geopotential height contours meandered widely around the Arctic region, indicating that the polar jet stream meandered similarly. In addition, the jet stream split into north and south branches over eastern Europe and the Russian far east, suggesting the existence of a blocking high. At 300 hPa, wave-activity fluxes (Figure 3a, green arrows) over the polar jet were oriented

from Europe to south of Alaska along the longitudinal circle, and they were particularly strong over eastern Europe and the Russian far east, suggesting Rossby wave sources in those areas. The existence of a double jet stream structure is also apparent in the two zonal wind maxima seen at about 72ºN and 45ºN along 135ºE (Figure 3c). From the surface to the upper troposphere at about 55ºN, where the largest negative wind anomaly is observed, the wind direction is easterly. This large-scale pattern in 2010 is consistent with the findings of Ogi et al. (2004), who reported an enhanced double jet in the positive phase of the summer AO.

3.1.2. Oceanic footprint left by the previous winter's negative AO

In the North Atlantic Ocean, a tripolar SST anomaly pattern, warm in the high latitudes, cool in the midlatitudes, and warm in the tropics, persisted from January to August 2010 (Figure 4). This tripolar pattern is typical of a negative wintertime NAO (e.g., Rodwell et al. 1999; Tanimoto and Xie 2002). In fact, the geopotential height anomaly field at 500 hPa in winter (DJF) 2009/2010 showed the typical pattern for the negative phase of the NAO (Figure 5). The strong negative phase of the AO index in the winter of 2009/2010 corresponded to the negative phase of the NAO (Figure 5a, b). The temperature anomaly at 850 hPa of winter in the region of high-latitude and mid-latitude North Atlantic corresponded well to the total latent and sensible heat flux anomaly in January and February (Figures. 4, 5c). Similar to the tripolar SST anomaly pattern, the total latent and sensible heat flux anomaly in January and February was also tripolar (Figure 4): a downward flux anomaly occurred over high latitudes and the tropical North Atlantic, and an upward flux anomaly was observed over the midlatitudes. The downward anomaly in the high latitudes and tropical North Atlantic lasted until April, but the sign of the latent and sensible heat flux anomaly reversed from downward to

upward over the tropical North Atlantic in May and June and over the North Atlantic high latitudes in July and August, whereas the warm SST anomaly in the high latitudes and tropical North Atlantic continued into the summer. The monthly mean tropical North Atlantic SST from January to August was the warmest observed in the 32 years from 1979 to 2010. On the strongly positive AO days, the OLR anomaly over the North Atlantic was strongly negative over the Caribbean Sea (Figure 6). The negative OLR anomaly area, which was characterized by strong convective activity, roughly coincided with the area of the warm SST and upward sensible and latent heat flux anomalies in summer. In addition, the wind field anomaly in the lower troposphere was cyclonic in the central area of the negative OLR anomaly in the tropical North Atlantic.

3.2. AGCM results

3.2.1 AO reproducibility of the AGCM EOF analysis

The EOF first mode for CTL is shown in Figure 7. This North-south dipole pattern is quite similar to that of SV NAM defined by Ogi et al (2004). Figure 8 shows the time series of the EOF in each run. All the time series start from negative value, implying that the results in the beginning is strongly influenced by the initial condition that is the same as in each run. About one month later, the time series of the index of each sensitivity run have a positive tendency except CTL. Only in the period of mid-August in only HAS was less than 0σ. In particular, the positive index value of AS was large in early August. In late August, the index of LAS was the largest. The average in August was the highest in AS and was 0.56σ. The average value of HAS and LAS in August were less than 0.5σ. The index of AS exceeded 0.5σ from 4 August. The index of HAS exceeded 0.5σ from 16 August. The index of LAS exceeded 0.5σ from 14 August. These positive departures of the AO index from CTL signify the SST anomaly

over the Atlantic consistently increases the score of the AO index.

3.2.2 The response of the atmosphere by North Atlantic SST

Figure 9 shows the monthly mean horizontal maps of 300 hPa geopotential height anomaly of the sensitivity runs from the CTL in August. In AS run, significant positive geopotential height anomalies at 300 hPa are seen over the northern and western North American continent, Norwegian Sea, Okhotsk Sea. The significant negative geopotental height anomalies are seen over North Pole and the North American continent. Wave activity fluxes emanate from the Okhotsk Sea and flow to the northern and western North American continent (Figure 9a). In HAS, significant positive geopotential height anomalies at 300 hPa are seen over the northern North American continent, Norwegian Sea, the Russian Far East and the Okhotsk Sea. The significant negative geopotential height anomalies are seen over North Pole and the eastern North American continent. Wave activity fluxes appear over the areas of the significant positive geopotential height anomalies. In particular, large fluxes emanate from the northern North American continent (Figure 9b). In LAS, significant positive geopotential height anomalies at 300 hPa are seen over the western North American continent, Norwegian Sea, the center of the Eurasian Continent and Hokkaido. The significant negative geopotential height anomalies are seen over North Pole, North American continent, North Atlantic Ocean and Karskoye More. Wave activity fluxes appear over the western North American continent and Norwegian Sea (Figure 9c).

Figure 10 shows the sum of latent heat flux and sensible heat flux anomaly from CTL averaged in August. Warm SST areas are upward fluxes. The upward flux of LAS is extending to high latitude area although the SST change in the LAS run is only in the low latitudes.

To examine the relationship between the anomalous upward flux area and the significant geopotential height anomaly areas, we examined the vertical cross section of geopotential height along 60ºN in August (Figure 11). Although significant areas cannot be seen in Figure 11c, the negative geopotential height anomalies are seen in the area of upward flux anomalies by every run. The positive geopotential height anomalies are seen next to the negative anomalies. The positive anomalies are significant in AS and HAS.

4. Discussion

Taking together the results of reanalysis data sets analysis in Section 3.1, we suggest that an oceanic memory of the strongly negative wintertime AO may have influenced the strongly positive summertime AO. A negative wintertime NAO would cause warm SST anomalies in high and low latitude regions of the Atlantic, as suggested by Xie and Tanimoto (1998) and Tanimoto and Xie (2002). Because the horizontal structures of the NAO and the AO in the Atlantic sector in winter 2009/2010 are similar (See Figure 5), the strongly negative wintertime AO would maintain the warm SST anomaly in this region. The high latitudes and the tropical Atlantic (Figure 4) in winter and spring indicates that anomalous heating of the ocean by the atmosphere occurred from winter to spring during the strongly negative phase of the AO in winter 2009/2010. Because the thermal heat capacity of the ocean is large, the sea surface stored this warmth (i.e., the SST anomaly remained positive) into the following summer.

In May and June, the heat flux anomaly changed from downward to upward in the tropics (see Figure 4), and in July and August, the center of the upward anomaly moved westward. The area of the upward heat flux anomaly coincided with the area of the warm SST anomaly from May to August. The warm SST during the summer following the strongly negative wintertime AO therefore heated the atmosphere, activating atmospheric convection. The OLR anomalies also indicate high convective activity in the tropical Atlantic region (Figure 6), suggesting a remote influence of the Atlantic SST upon the occurrence of an anticyclone over Europe. This Atlantic SST influence has been pointed out by many studies (e.g., Cassou et al. 2005; García-Serrano et al. 2008). García-Serrano et al. (2008) showed that a midlatitude anticyclonic anomaly related to tropical convection can excite a Rossby wave. Weak, positive OLR anomalies along the Gulf Stream were associated with anticyclonic

surface winds on strongly positive AO days (Figure 6). The observed wave activity flux (Figure 3a) also seems to emanate from that region. This midlatitude signature implies that strengthening of the positive geopotential anomalies over Europe was associated with the Atlantic tripolar SST anomaly.

The positive geopotential anomaly in the area of the polar jet stream caused eastward propagation of Rossby waves, and the unusual amplification of Rossby waves might have led to the formation of blocking anticyclones. These findings are in agreement with previous studies. For example, Tachibana et al. (2010) reported that a blocking anticyclone over the Atlantic sector that induces blocking over the Russian Far East is associated with a long-lasting, strongly positive AO caused by wave–mean flow interactions. As a result of these interactions, the positive AO pressure pattern can continue for a long time. In addition, Orsolini and Nikulin (2006) pointed out that the blocking anticyclone over Europe in summer 2003 was part of a wave train extending from Europe to eastern Eurasia.

Taking together the results of AFES shown in Section 3.2 and the observation analysis, we suggest that the North Atlantic SST in July and August 2010 may have influenced the strongly positive summertime AO. Because AO jumped positive and kept positive until the end of August in all the runs in which the North Atlantic SSTs were changed to those of July and August 2010, the positive AO occurred is under the influence of the SST anomaly of the North Atlantic Ocean. Because cyclonic anomalies are seen in upward sensible and latent heat flux areas, the cyclonic anomalies could be formed by the anomalous heat fluxes. The cyclonic anomalies induce anticyclone anomalies leeward of the westerlies. Although the anticyclonic anomaly is not over Europe, the anomalies can be induced by Rossby wave, and propagate the anomalies to other areas.

Of course, the set of processes introduced here is just one possible explanation for the formation of the strongly positive summer AO in 2010. For example, summer time SST anomalies in the Mediterranean Sea (Feudale and Shukla 2010) might simultaneously induce a strongly positive summer AO. Although the effect of the oceanic memory of a negative AO during the previous winter might be smaller than the effects of simultaneous events, the previous winter's footprint may at least play a role in the reversal of the AO polarity from a strongly negative wintertime AO to a strongly positive summertime AO. If this reversal pattern recurs, it might be possible to predict the summer AO from the wintertime AO. The more negative the winter AO anomaly is, the deeper the footprint left in the ocean would be, suggesting that a winter-to-summer reversal of the AO might occur only in years when the negative wintertime AO anomaly is large. In addition to an oceanic memory effect, other memory effects such as anomalous snow accumulation on the Eurasian continent or elsewhere in the Northern Hemisphere, as suggested by Ogi et al. (2003) and Barriopedro et al. (2006), may also contribute to the reversal of AO polarity. To test these possibilities, additional experiment of AGCM is the next step.

Acknowledgment

I express gratitude to Professor Tachibana, my supervisor. He taught me the basic knowledge of the physics and detailed knowledge of the physical oceanography and the atmospheric dynamics. Additionally, many professors of Geosystem Science, Graduate school of Bioresources, Mie University advised me. I thank that very much.

Tetsu Nakamura of the National Institute of Polar Research taught me the EOF analysis of SV NAM, the wave activity flux. I thank Akira Yoshida and Akira Yamazaki of Earth Simulator, Japan Agency for Marine-Earth Science and Technology taught me the AFES. I was helped by their advices. I express gratitude to them.

Members of climate and ecosystems dynamics laboratory provided some advices for my research. In particular, I got a lot of assistance from the students of doctoral course. I would like to thank for them.

References

Barriopedro, D., R. García-Herrera, and E. Hernández (2006), The role of snow cover in the Northern Hemisphere winter to summer transition, *Geophys. Res. Lett.*, **33**, L14708, doi:10.1029/2006GL025763.

Barriopedro, D., E.M. Fischer, J. Luterbacher, R.M. Trigo, and R. García-Herrera (2011), The hot summer of 2010: redrawing the temperature record map of Europe, *Science*, **332**, 220–224, doi:10.1126/science. 1201224.

Cassou, C., L. Terray, and A.S. Phillips (2005), Tropical Atlantic influence on European heat waves, *J. Clim.*, **18**, 2805–2811.

Cattiaux, J., R. Vautard, C. Cassou, P. Yiou, V. Masson-Delmotte, and F. Codron (2010), Winter 2010 in Europe: a cold extreme in a warming climate, *Geophys. Res. Lett.*, **37**, L20704, doi:10.1029/2010GL 044613.

Feudale, L. and J. Shukla (2010), Influence of sea surface temperature on the European heat wave of 2003 summer. Part I: an observational study, *Clim. Dyn.*, **36**, 1691–1703, doi:10.1007/s00382-010-0788-0.

García-Serrano, J., T. Losada, B. Rodríguez-Fonseca, and I. Polo (2008), Tropical Atlantic variability modes (1979–2002). Part II: timeevolving atmospheric circulation related to SST-forced tropical convection, *J. Clim.*, **24**, 6476–6497.

Kalnay, E. et al (1996), The NCEP/NCAR 40 year reanalysis project, *Bull. Am. Meteorol. Soc.*, **77**, 437–471.

Liebmann, B. and C.A. Smith (1996), Description of a complete (interpolated) outgoing longwave radiation dataset, *Bull. Am. Meteorol. Soc.*, **77**, 1275–1277.

Matsueda, M. (2011), Predictability of Euro-Russian blocking in summer of 2010, *Geophys. Res. Lett.*, **38**, L06801, doi:10.1029/2010GL 046557.

Ogi, M., K. Yamazaki and Y. Tachibana (2003), Solar cycle modulation of the seasonal

linkage of the North Atlantic Oscillation (NAO), *Geophys. Res. Lett.*, **30**, 2170, doi:10.1029/2003GL018545.

Ogi, M., K. Yamazaki, Y. Tachibana (2004), The summertime annular mode in the Northern Hemisphere and its linkage to the winter mode, *J. Geophys. Res.*, **109**, D20114, doi:10.1029/2004JD004514.

Ogi, M., K. Yamazaki and Y. Tachibana (2005), The summer northern annular mode and abnormal summer weather in 2003, *Geophys. Res. Lett.*, **32**, L04706, doi:10.1029/2004GL021528.

Onogi, K. et al (2007), The JRA-25 reanalysis, *J. Meteorol. Soc. Japan*, **85**, 369–432.

Orsolini, Y.J. and G. Nikulin (2006), A low-ozone episode during the European heatwave of August 2003, *Quart. J. R. Meteor. Soc.*, **615**, 667–680, doi:10.1256/qj.05.30.

Rodwell, M.J., D.P. Rowell and C.K. Folland (1999), Oceanic forcing of the wintertime North Atlantic Oscillation and European climate, *Nature*, **398**, 320–323.

Smith, T.M., R.W. Reynolds, T.C. Peterson, and J. Lawrimore (2008), Improvements to NOAA's historical merged land-ocean surface temperature analysis (1880–2006), *J. Clim.*, **21**, 2283–2296.

Tachibana, Y., T. Nakamura, H. Komiya, and M. Takahashi (2010), Abrupt evolution of the summer Northern Hemisphere annular mode and its association with blocking, *J. Geophys. Res.*, **115**, D12125, doi:10.1029/2009JD012894.

Takaya, K. and H. Nakamura (2001), A formulation of a phase-independent wave-activity flux for stationary and migratory quasigeostrophic eddies on a zonally varying basic flow, *J. Atmos. Sci.*, **58**, 608–627.

Tanimoto, Y., S.P. Xie (2002), Inter-hemispheric decadal variations in SST, surface wind, heat flux and cloud cover over the Atlantic Ocean, *J. Meteor. Soc. Japan*, **80**, 1199–

1219.

Thompson, D.W.J. and J.M. Wallace (2000), Annular modes in the extratropical circulation. Part I: month-to-month variability, *J. Clim.*, **13**, 1000–1016.

Trigo, R.M., R. García-Herrera, J. Díaz, I.F. Trigo, and M.A. Valente (2005), How exceptional was the early August 2003 heatwave in France?, *Geophys. Res. Lett.*, **32**, L10701, doi:10.1029/2005GL022410.

Wang, L. and W. Chen (2010), Downward Arctic Oscillation signal associated with moderate weak stratospheric polar vortex and the cold December 2009, *Geophys. Res. Lett.*, **37**, L09707, doi:10.1029/2010GL042659.

Xie, S.P. and Y. Tanimoto (1998), A Pan-Atlantic decadal climate oscillation, *Geophys. Res. Lett.*, **25**, 2185–2188.

Xue, Y., T.M. Smith, and R.W. Reynolds (2003), Interdecadal changes of 30 year SST normals during 1871-2000, *J. Clim.*, **16**, 1601–1612.

Figure captions

Figure 1 (Top) Time series of the AO index (blue) as defined by Ogi et al. (2004), who called it the SV NAM index. For reference, the conventional AO index reported by NOAA/CPC is shown by the gray line. The vertical axis is dimensionless because the indices are normalized. Tick marks on the horizontal axis indicate the 1 day of each month. Updated daily time series from 1958 are available at http://www.bio.mie-u.ac.jp/kankyo/shizen/lab1/AOindex.htm. (Bottom) Time series of the temperature anomaly (K) at 925 hPa averaged northward of 32.5ºN over the Eurasian continent. Anomalies are calculated according to the daily climatology of 32 years.

Figure 2 SST (ºC) of July and August 2010. Color area is the area which changes a boundary condition in AS.

Figure 3 a Time-mean geopotential height at 300 hPa, b temperature at 850 hPa (T850), and c vertical cross section of the eastward wind component at 135ºE in the Northern Hemisphere during strongly positive AO days from 10 July to 4 August 2010. Contours show time-mean values of geopotential height (a, contour interval 100 m), temperature (b, contour interval 5 K), and wind speed (c, contour interval 5 m s^{-1}), and the color shading shows (a) the geopotential height anomaly, (b) the temperature anomaly, and (c) the zonal wind anomaly from climatological temporal means. The green arrows in (a) show the wave activity flux (m^2 s^{-2}) at 300 hPa as formulated by Takaya and Nakamura (2001), with the scale shown by the arrow in the upper right corner.

Figure 4 Evolution of (left column) SST and its anomaly, and (right column) the sum of the latent and sensible heat fluxes and its anomaly, from January to August 2010. Contours show 2 month mean values, and the color shading shows the anomalies (deviations from the climatological temporal mean). JF, January and February; MA, March and April; MJ, May and June; JA, July and August. The contour interval for SST is 3ºC, and that for the flux is 40 W m^{-2}. Here, a positive flux (i.e., upward flux) is defined as from the ocean to the atmosphere. Red or blue shading in the right panels thus indicates anomalous heating or cooling of the ocean, respectively.

Figure 5 Winter 2009/2010 (December, January, and February) mean geopotential height at 1000 hPa (a) and 500 hPa (b) and temperature at 850 hPa (c). Contours show winter mean values of geopotential height (contour interval 50 m) and temperature (contour interval 5 K). The color shading shows the geopotential height anomaly or the temperature anomaly from climatological temporal means.

Figure 6 OLR anomaly (color scale, W m^{-2}), defined as the deviation from the climatological temporal mean, on strongly positive AO days. Arrows show the surface wind anomaly (m s^{-1}) on strongly positive AO days, with the scale shown by the arrow below the lower right corner.

Figure 7 The vertical cross section of the eigenvector of the leading mode in August by an EOF analysis for the CTL run.

Figure 8 Time series of EOF first mode indexes. Gray bar is CTL. Red line is AS. Yellow line is HAS. Blue line is LAS.

Figure 9 300 hPa geopotential height in (a) AS, (b) HAS and (c) LAS August. Color is significance. Contour is anomaly (m) from CTL. Arrows are wave activity flux (m^2 s^{-2}).

Figure 10 The sum of latent and sensible heat flux anomaly from CTL in August average. (a) AS, (b) HAS, (c) LAS.

Figure 11 Vertical cross section of the geopotential height (m) at 60^{O}N in August average. (a) AS, (b) HAS, (c) LAS. Color is significance. Contour is anomaly from CTL.

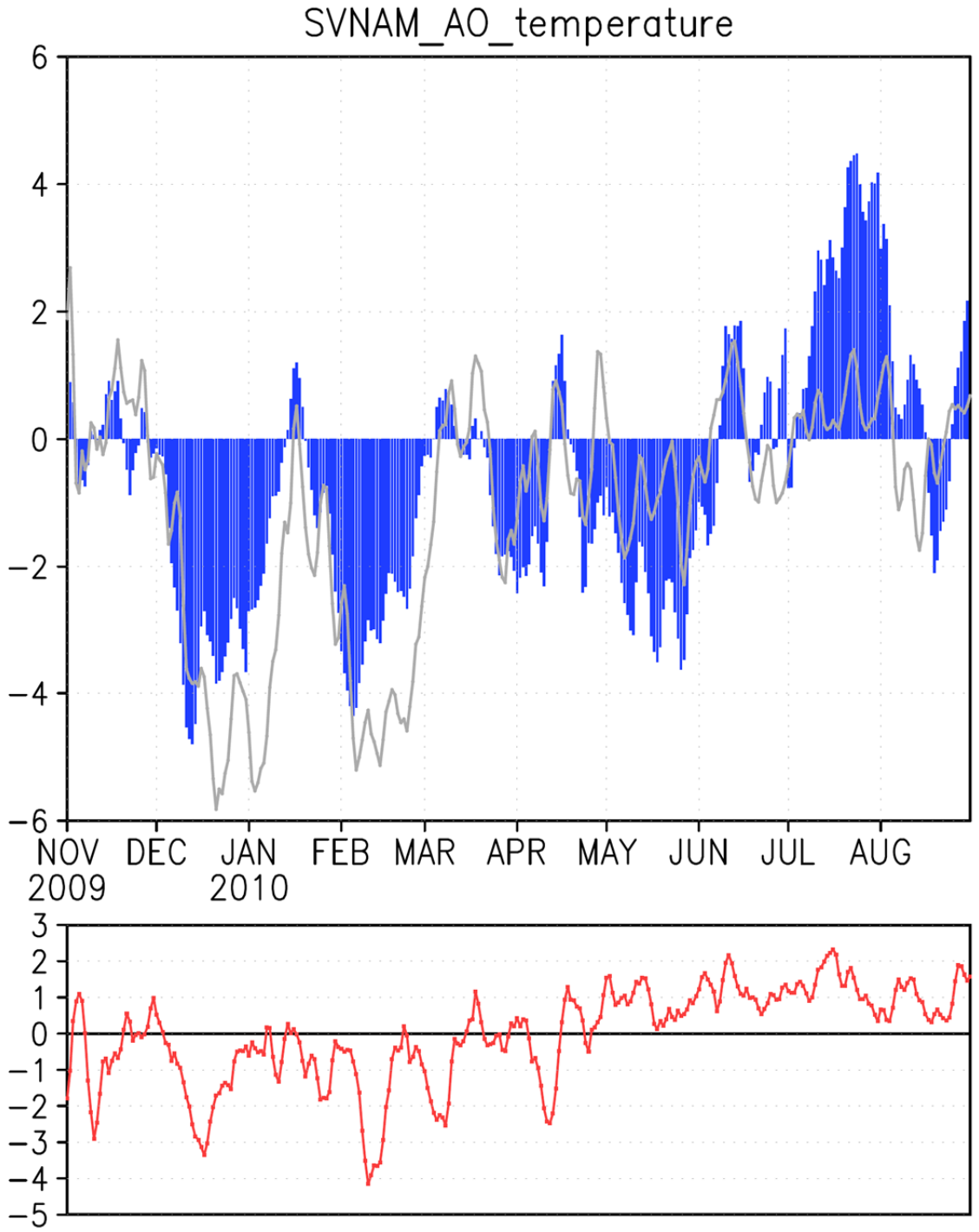

Figure 1 **(Top) Time series of the AO index (blue) as defined by Ogi et al. (2004), who called it the SV NAM index. For reference, the conventional AO index reported by NOAA/CPC is shown by the gray line. The vertical axis is dimensionless because the indices are normalized. Tick marks on the horizontal axis indicate the 1 day of each month. Updated daily time series from 1958 are available at http://www.bio.mie-u.ac.jp/kankyo/shizen/lab1/AOindex.htm. (Bottom) Time series of the temperature anomaly (K) at 925 hPa averaged northward of 32.5ºN over the Eurasian continent. Anomalies are calculated according to the daily climatology of 32 years.**

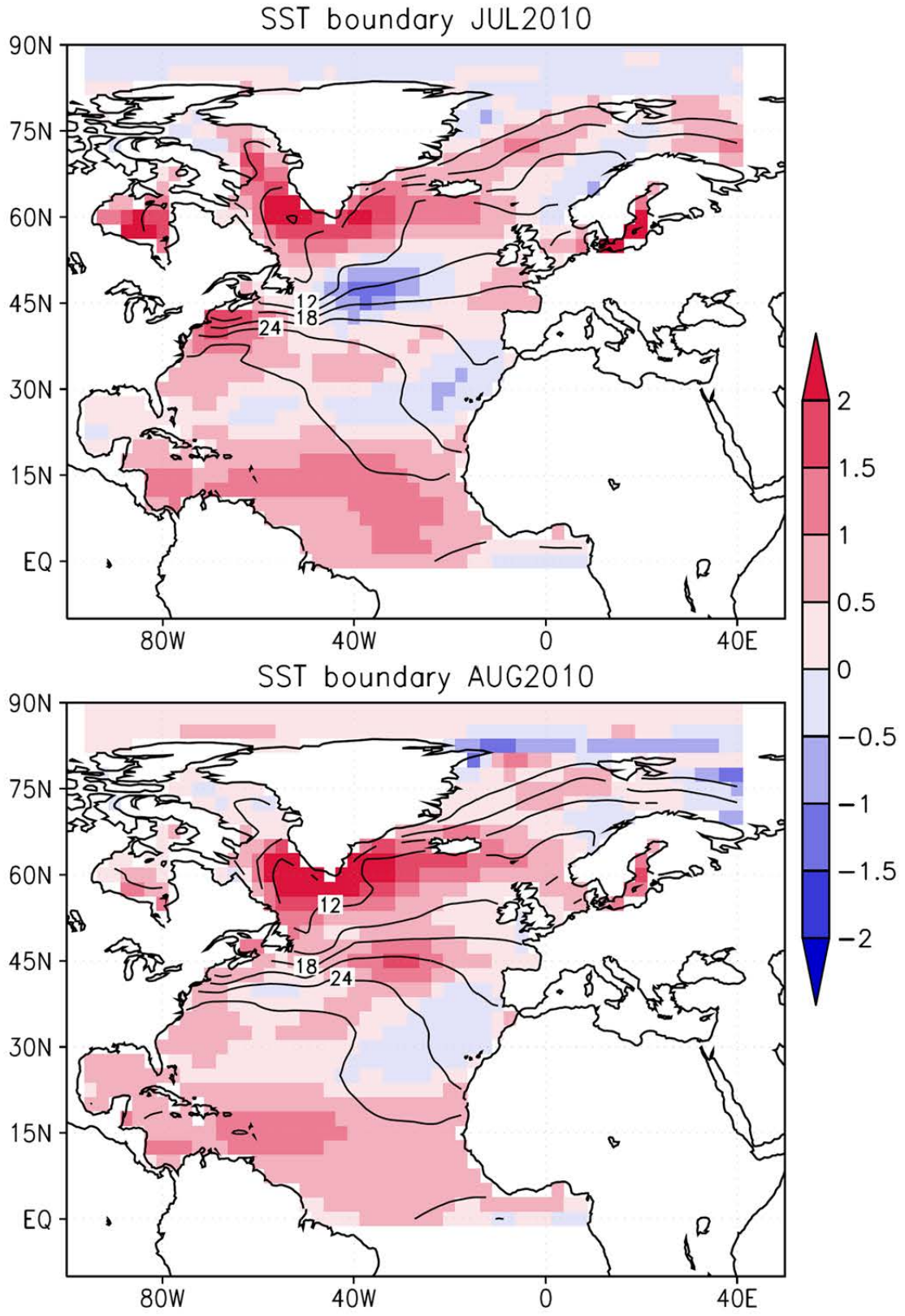

Figure 2 SST (ºC) of July and August 2010. Color area is the area which changes a boundary condition in AS.

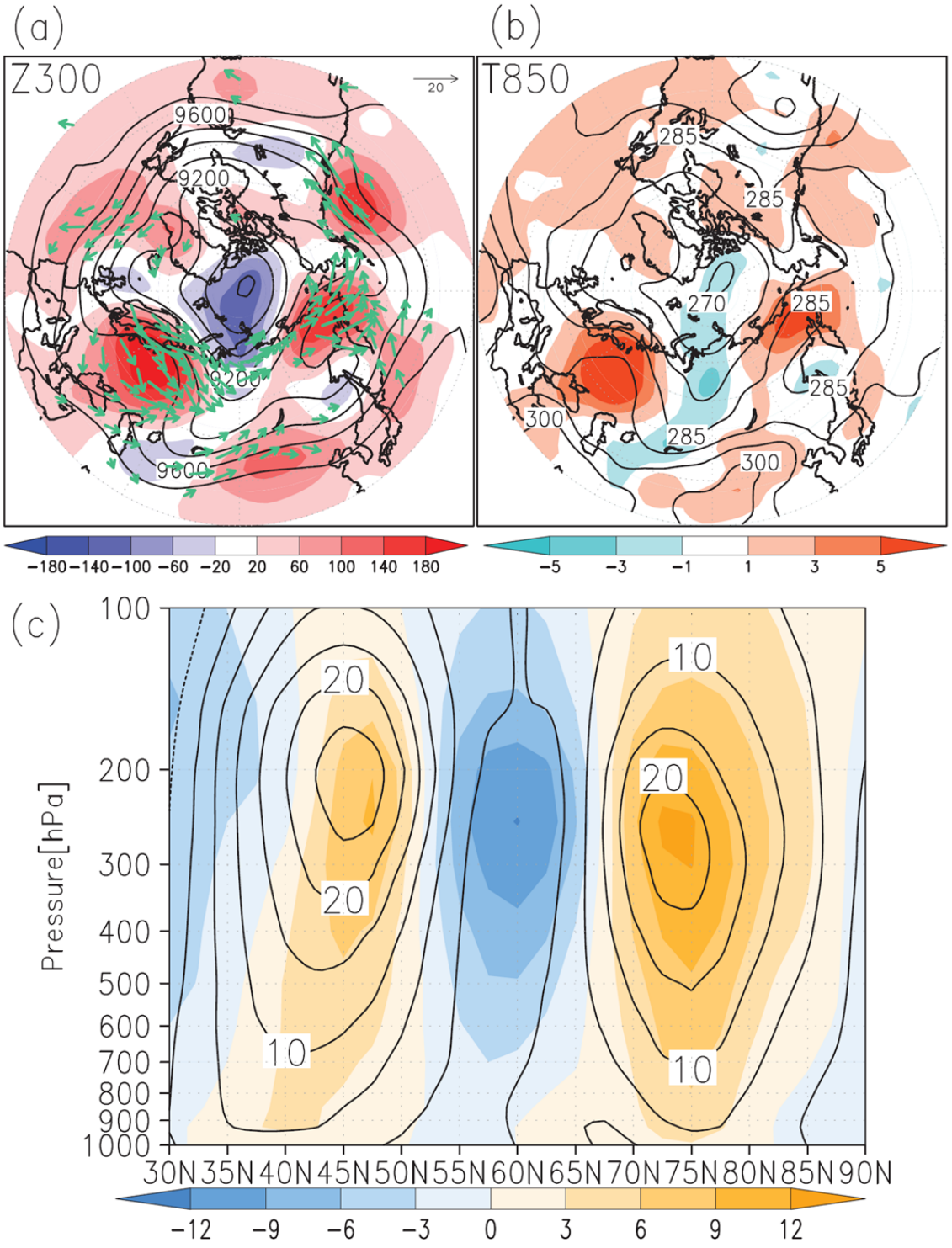

Figure 3 **a Time-mean geopotential height at 300 hPa, b temperature at 850 hPa (T850), and c vertical cross section of the eastward wind component at 135ºE in the Northern Hemisphere during strongly positive AO days from 10 July to 4 August 2010. Contours show time-mean values of geopotential height (a, contour interval 100 m), temperature (b, contour interval 5 K), and wind speed (c, contour interval 5 m s^{-1}), and the color shading shows (a) the geopotential height anomaly, (b) the temperature anomaly, and (c) the zonal wind anomaly from climatological temporal means. The green arrows in (a) show the wave activity flux (m^2 s^{-2}) at 300 hPa as formulated by Takaya and Nakamura (2001), with the scale shown by the arrow in the upper right corner.**

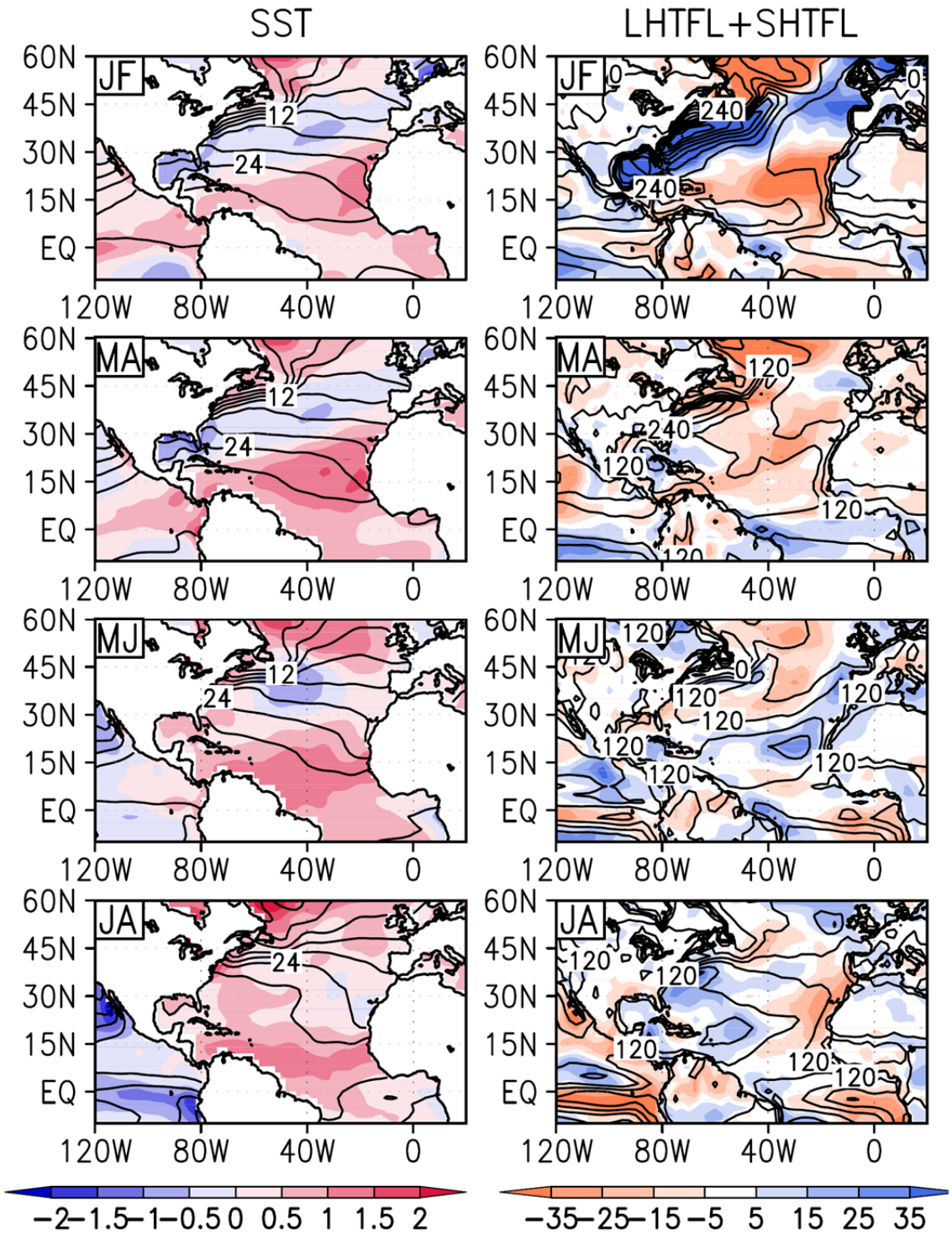

Figure 4 **Evolution of (left column) SST and its anomaly, and (right column) the sum of the latent and sensible heat fluxes and its anomaly, from January to August 2010. Contours show 2 month mean values, and the color shading shows the anomalies (deviations from the climatological temporal mean). JF, January and February; MA, March and April; MJ, May and June; JA, July and August. The contour interval for SST is 3ºC, and that for the flux is 40 W m^{-2}. Here, a positive flux (i.e., upward flux) is defined as from the ocean to the atmosphere. Red or blue shading in the right panels thus indicates anomalous heating or cooling of the ocean, respectively.**

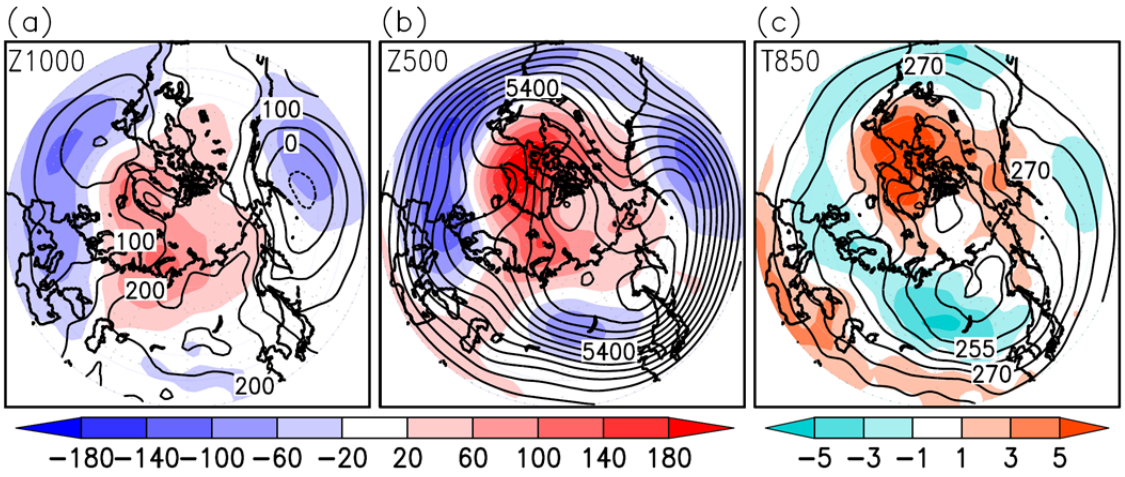

Figure 5 Winter 2009/2010 (December, January, and February) mean geopotential height at 1000 hPa (a) and 500 hPa (b) and temperature at 850 hPa (c). Contours show winter mean values of geopotential height (contour interval 50 m) and temperature (contour interval 5 K). The color shading shows the geopotential height anomaly or the temperature anomaly from climatological temporal means.

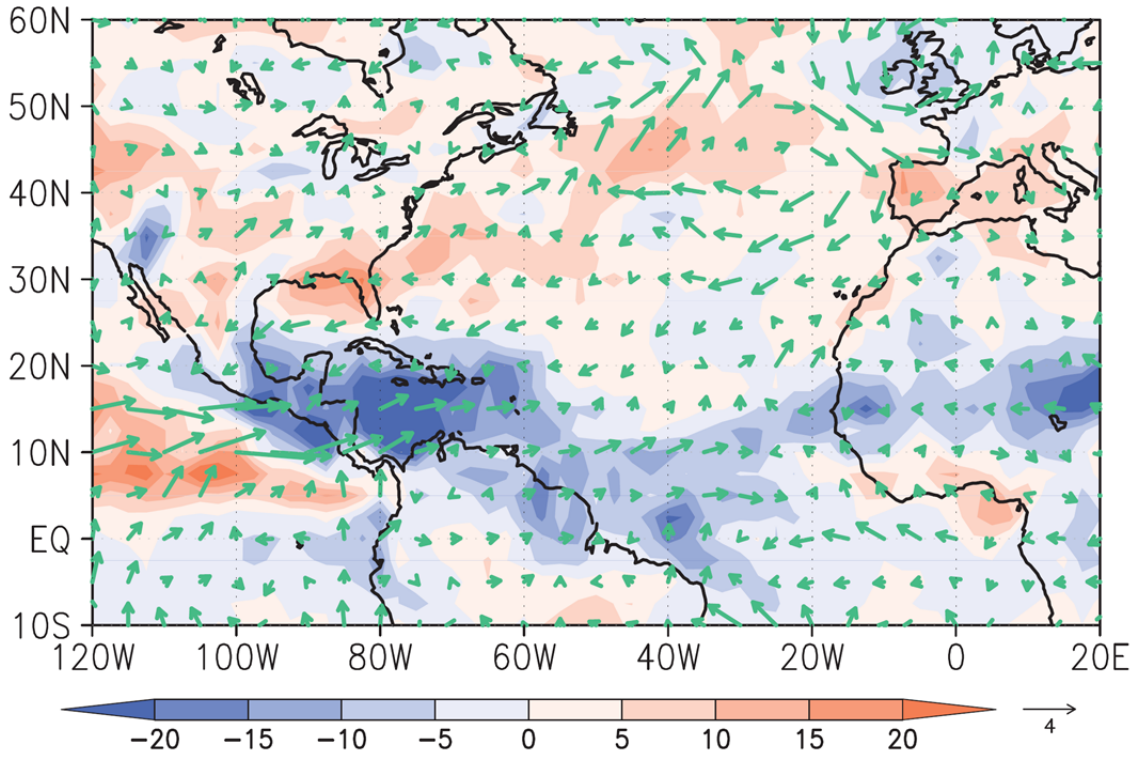

Figure 6 OLR anomaly (color scale, W m^{-2}), defined as the deviation from the climatological temporal mean, on strongly positive AO days. Arrows show the surface wind anomaly (m s^{-1}) on strongly positive AO days, with the scale shown by the arrow below the lower right corner.

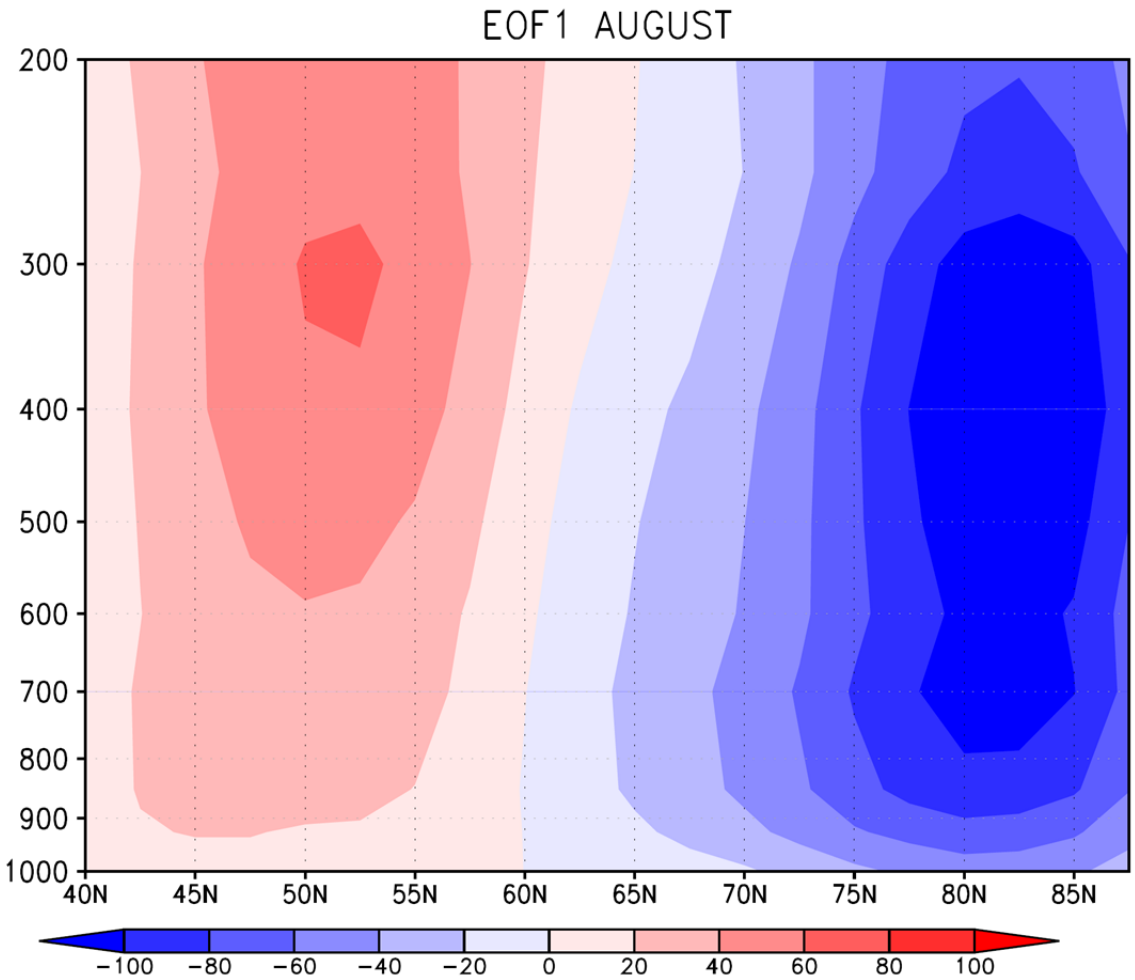

Figure 7 The vertical cross section of the eigenvector of the leading mode in August by an EOF analysis for the CTL run.

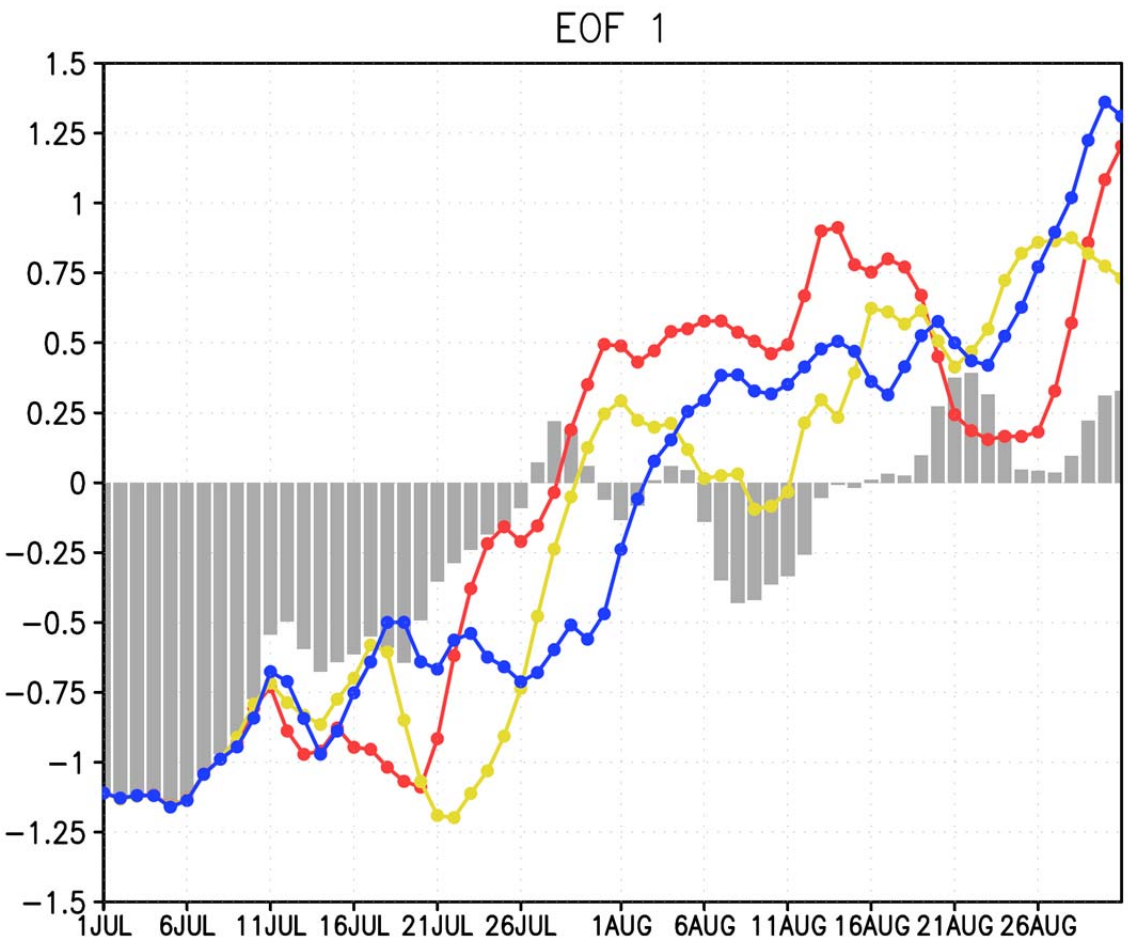

Figure 8 Time series of EOF first mode indexes. Gray bar is CTL. Red line is AS. Yellow line is HAS. Blue line is LAS.

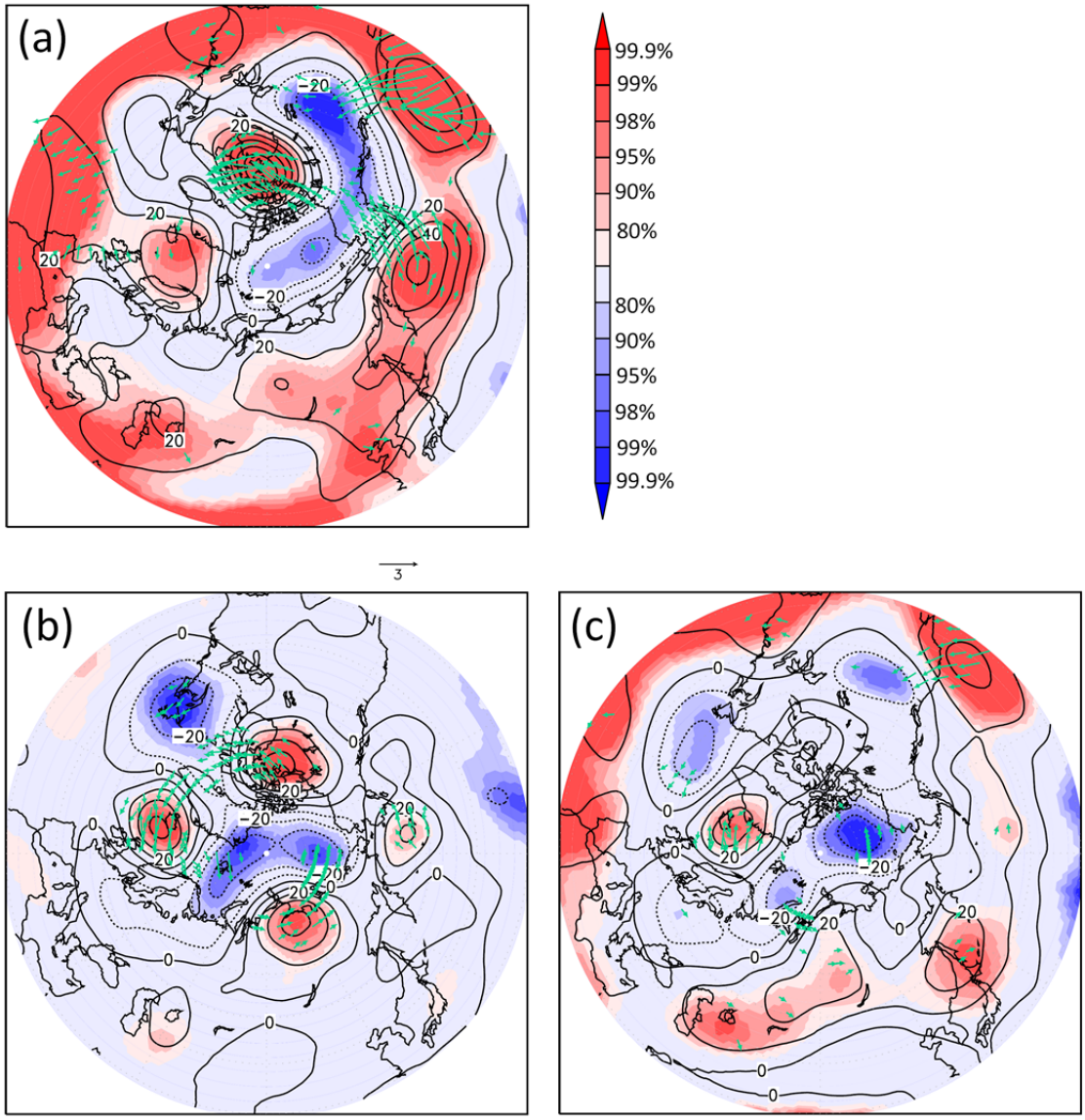

Figure 9 300 hPa geopotential height in (a) AS, (b) HAS and (c) LAS August. Color is significance. Contour is anomaly (m) from CTL. Arrows are wave activity flux (m^2 s^{-2}).

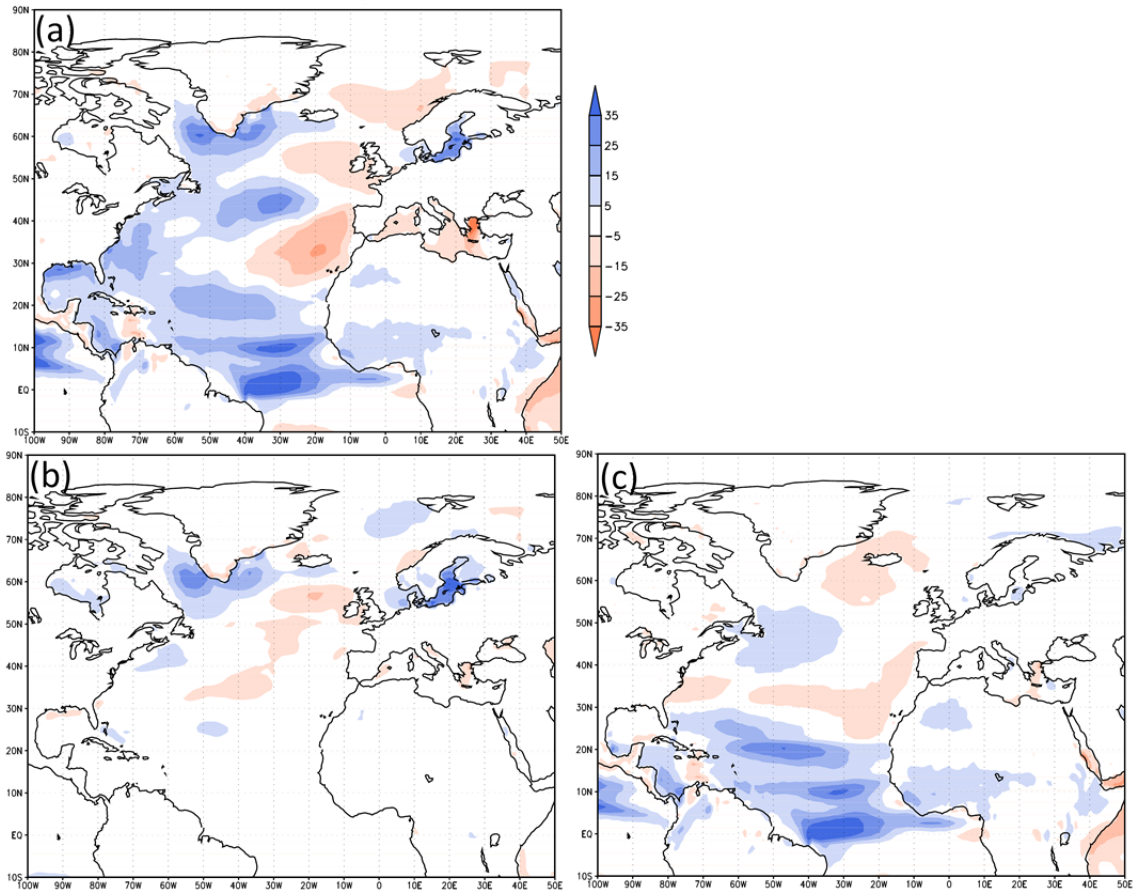

Figure 10 The sum of latent and sensible heat flux anomaly from CTL in August average. (a) AS, (b) HAS, (c) LAS.

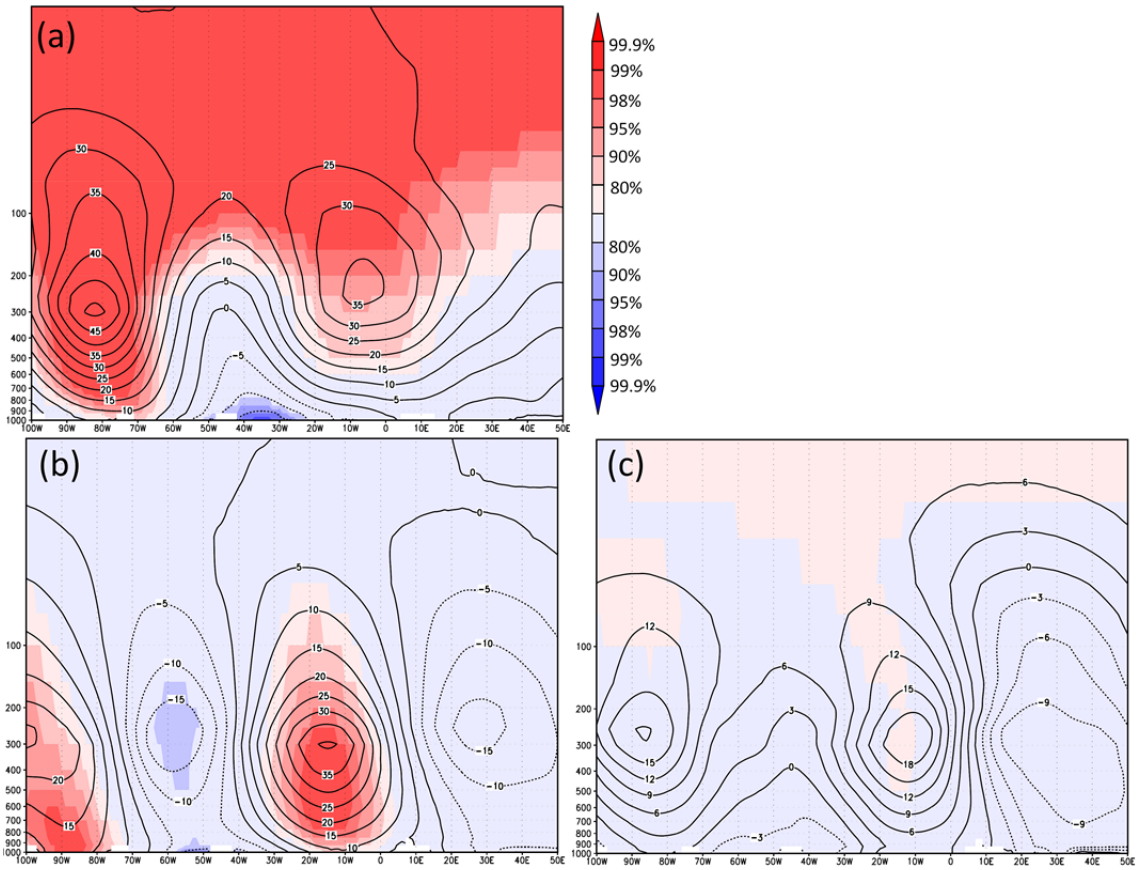

Figure 11 Vertical cross section of the geopotential height (m) at 60°N in August average. (a) AS, (b) HAS, (c) LAS. Color is significance. Contour is anomaly from CTL.